

Glaucoma secondary to vascular changes in optic nerve head, retina, and choroid: abridged secondary publication

CCY Tham *, PPM Chan, CYL Cheung, DYL Leung, NCY Chan, CWY Chow

KEY MESSAGES

1. Decreased vessel density is associated with impaired visual sensitivity in the early stage of normal-tension glaucoma.
2. Patterns of retinal vasculature changes differ between normal-tension glaucoma and primary angle-closure glaucoma.
3. Lower retinal vasculature density at baseline is associated with faster progression of normal-tension glaucoma.
4. Vascular changes develop prior to retinal nerve fibre layer (RNFL) thinning in normal-tension

glaucoma, whereas RNFL thinning develops prior to vascular changes in primary angle-closure glaucoma.

Hong Kong Med J 2024;30(Suppl 1):S40-44

HMRF project number: 05162836

CCY Tham, PPM Chan, CYL Cheung, DYL Leung, NCY Chan, CWY Chow

Department of Ophthalmology and Visual Sciences, The Chinese University of Hong Kong, Hong Kong SAR, China

* Principal applicant and corresponding author: clemtham@cuhk.edu.hk

Introduction

Glaucoma is a major cause of irreversible blindness worldwide.¹ It is characterised by retinal ganglion cell (RGC) degeneration, which results in thinning of the optic disc and retinal nerve fibre layer (RNFL) as well as visual field loss. The pathogenesis of glaucoma remains unknown. Intraocular pressure (IOP) reduction is the only effective therapeutic strategy to slow glaucoma progression, but some patients experience continued progression despite clinically significant IOP reduction.

Various vascular mechanisms such as decreased perfusion pressure, vascular dysregulation, and vasospasm may involve in the pathogenesis and progression of glaucoma.^{2,3} Both IOP and vascular factors are likely to cause high-tension glaucoma (primary open-angle glaucoma and primary angle-closure glaucoma [PACG]) and normal-tension glaucoma (NTG). Retinal arteriolar narrowing is associated with the 10-year incidence of glaucoma, independent of IOP and ocular perfusion pressure.⁴

Optical coherence tomography angiography (OCT-A) enables quantitative evaluation of retinal and choroidal microvasculature. Microvascular reduction is associated with visual field defects and RGC loss in glaucoma. We used OCT-A to quantify capillary networks and evaluate the causal relationship between retinal vascular changes and RGC loss in glaucoma.

Methods

This study was conducted from 1 April 2018 to 31 July 2022. Patients with glaucoma and healthy controls were consecutively recruited for ophthalmic examinations of visual acuity, IOP, refraction, axial length, and visual field, using dark-room gonioscopy, OCT, and OCT-A imaging. All patients with glaucoma were followed up every 6 months.

OCT-A imaging was performed using a volume scan over a 3×3-mm macular region centred on the optic nerve head and the fovea. In the macular region, only the superficial capillary plexus was analysed because the deep capillary plexus can be affected by shadow graphical projection artefacts from the superficial capillary plexus. In the optic disc region, only the radial peripapillary capillary layer was analysed because this layer contains the blood supply for the RNFL layer. A customised MATLAB programme was used to process OCT-A images and generate a series of quantitative OCT-A metrics. Multiple quantitative vascular parameters were generated, including vessel density (VD), fractal dimension, and vessel diameter index.

For cross-sectional analyses, generalised estimating equations were used to correct for inter-eye correlations. Linear regression was performed to examine associations between OCT-A metrics and glaucoma parameters. For longitudinal analysis, the rates of change in VD and RNFL thickness were

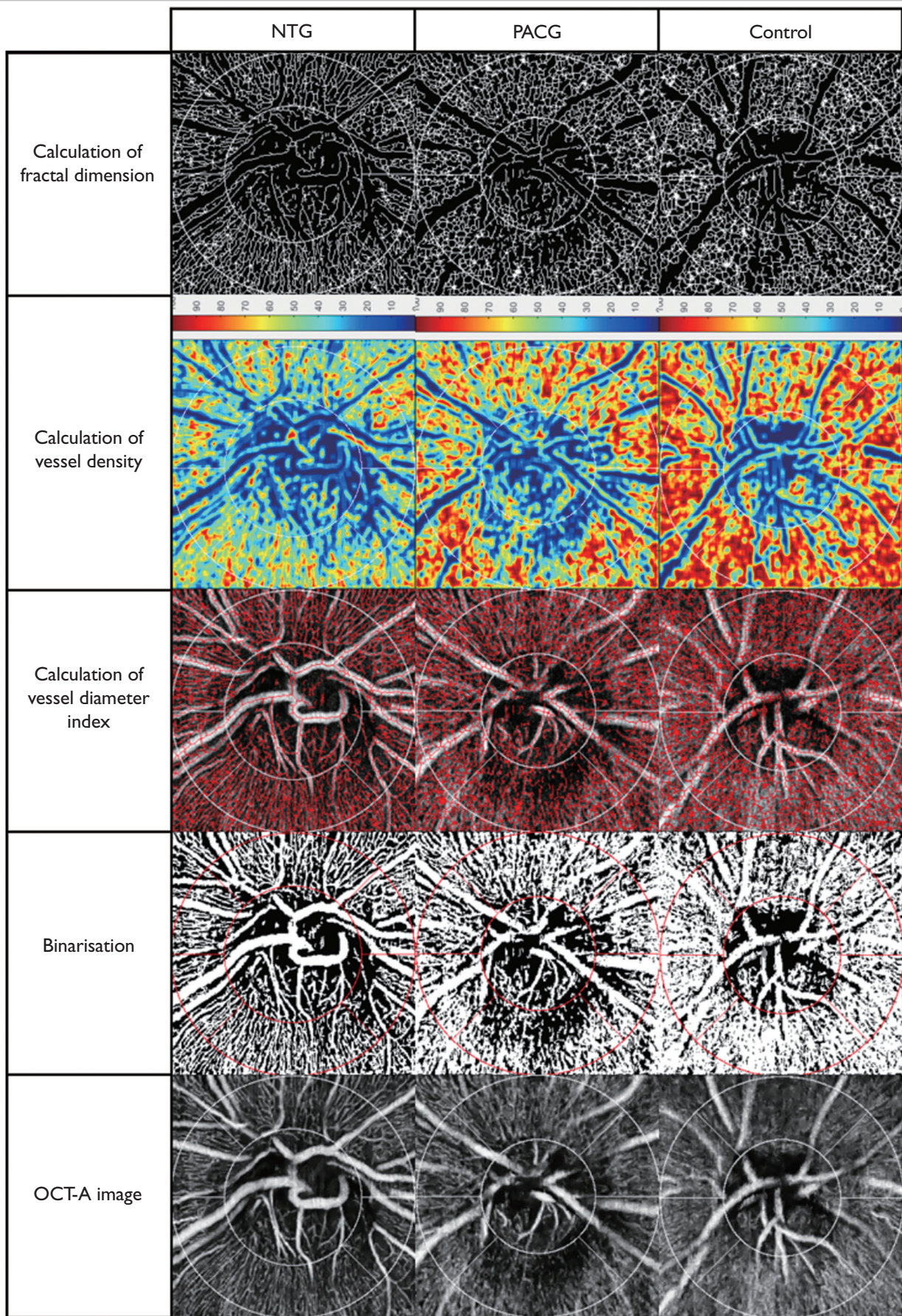


FIG. Quantitative peripapillary microvasculature metrics in optical coherence tomography angiography (OCT-A) images of patients with normal-tension glaucoma (NTG), patients with primary angle-closure glaucoma (PACG), and healthy controls.

TABLE 1. Associations of circumpapillary vessel density (VD) and circumpapillary fractal dimension (FD) with mean retinal nerve fibre layer (RNFL) thickness

Metric	Univariable model*		Multivariable model*	
	RNFL thickness, μm	P value	RNFL thickness, μm	P value
Patients with primary angle-closure glaucoma				
Circumpapillary VD, %	-5.855 (-9.567 to -2.143)	0.002	-4.242 (-8.120 to -0.363)	0.032
Circumpapillary FD	-9.297 (-11.682 to -6.913)	<0.001	-8.894 (-11.925 to -5.864)	<0.001
Patients with normal-tension glaucoma				
Circumpapillary VD, %	-4.998 (-7.674 to -2.322)	<0.001	-5.531 (-9.472 to -1.590)	0.006
Circumpapillary FD	-9.831 (-15.901 to -3.761)	0.002	-12.064 (-17.195 to -6.932)	<0.001
Controls				
Circumpapillary VD, %	1.918 (-0.684 to 4.520)	0.148	2.221 (-0.197 to 4.638)	0.072
Circumpapillary FD	-0.646 (-3.284 to 1.992)	0.631	-1.325 (-3.891 to 1.241)	0.312

* Data are presented as mean (95% confidence interval) per standard-deviation decrease

TABLE 2. Age- and baseline measurement-adjusted rates of change in vessel density and retinal nerve fibre layer thickness

Variables	Patients with normal-tension glaucoma*	P value	Patients with primary angle-closure glaucoma*	P value	Difference*	P value
Vessel density, %/y						
Global	-1.65 (-2.40 to -0.89)	<0.001	-0.66 (-1.32 to -0.01)	0.047	-1.08 (-1.90 to -0.27)	0.009
Temporal	-2.06 (-3.08 to -1.05)	<0.001	-0.49 (-1.36 to 0.38)	0.262	-1.57 (-2.91 to -0.23)	0.022
Superotemporal	-2.23 (-3.39 to -1.08)	<0.001	-0.75 (-1.76 to 0.26)	0.140	-1.46 (-2.65 to -0.26)	0.017
Inferotemporal	-1.63 (-2.77 to -0.49)	0.006	-0.73 (-1.73 to 0.26)	0.143	-0.99 (-2.23 to 0.25)	0.117
Superonasal	-1.09 (-2.19 to 0.00)	0.050	-0.46 (-1.54 to 0.61)	0.394	-0.86 (-2.09 to 0.38)	0.172
Inferonasal	-1.61 (-2.80 to -0.41)	0.009	-1.25 (-2.58 to 0.09)	0.067	-0.67 (-2.03 to 0.69)	0.334
Nasal	-1.39 (-2.37 to -0.42)	0.006	-0.67 (-1.57 to 0.23)	0.138	-0.74 (-1.81 to 0.34)	0.178
Retinal nerve fibre layer thickness, $\mu\text{m}/\text{y}$						
Global	-0.25 (-0.92 to 0.43)	0.467	-0.62 (-1.14 to -0.10)	0.020	0.41 (-0.48 to 1.30)	0.360
Temporal	-0.33 (-1.10 to 0.44)	0.399	-0.45 (-1.03 to 0.13)	0.127	0.12 (-0.85 to 1.09)	0.801
Superotemporal	-1.11 (-2.06 to -0.17)	0.022	-0.43 (-1.34 to 0.48)	0.354	-0.72 (-2.03 to 0.58)	0.276
Inferotemporal	-1.76 (-2.79 to -0.73)	0.001	-0.97 (-1.79 to -0.16)	0.019	-0.63 (-1.95 to 0.68)	0.342
Superonasal	-0.89 (-1.59 to -0.18)	0.013	-0.96 (-1.82 to -0.11)	0.028	0.07 (-0.95 to 1.10)	0.889
Inferonasal	-0.75 (-1.75 to 0.25)	0.138	-0.84 (-1.70 to 0.01)	0.053	0.03 (-1.28 to 1.34)	0.969
Nasal	-0.30 (-1.35 to 0.75)	0.569	-0.37 (-0.95 to 0.20)	0.197	0.05 (-1.13 to 1.23)	0.933

* Data are presented as coefficient (95% confidence interval)

estimated by linear mixed-effects modelling. Mean differences in rates of change between diagnostic groups were compared by linear mixed-effects modelling.

Results

In total, 250 patients with NTG, 250 patients with PACG, and 130 healthy controls were recruited. Their quantitative peripapillary microvasculature metrics on OCT-A were compared (Fig). Decreased circumpapillary VD and circumpapillary fractal dimension were associated with decreased RNFL thickness in both NTG and PACG groups (all $P \leq 0.032$, Table 1). The associations between OCT-A metrics and RNFL thickness were stronger in the NTG group than in the PACG group.

In the NTG group, the rate of VD loss was significantly different from zero in each sector and global region (all $P \leq 0.05$); the rate of RNFL thinning was significantly different from zero in the superotemporal, inferotemporal, and superonasal sectors ($P \leq 0.022$) [Table 2]. In the PACG group, the rate of VD loss was significantly different from zero in the global region ($P = 0.047$); the rate of RNFL thinning was significantly different from zero in the inferotemporal and superonasal sectors as well as the global region (all $P \leq 0.028$). Compared with the PACG group, the NTG group had more rapid VD loss in the global region ($P = 0.009$), temporal sector ($P = 0.022$), and superotemporal sector ($P = 0.017$).

Discussion

We used OCT-A to compare peripapillary microvasculature between two subtypes of early glaucoma with different pathogeneses: NTG is less IOP-dependent and has a stronger vascular pathogenic component, whereas PACG is more IOP-dependent.⁵ Global circumpapillary VD was significantly reduced in NTG eyes, compared with PACG eyes, despite comparable RNFL thickness and disease severity. Furthermore, NTG eyes exhibited significantly lower circumpapillary VDs in the inferotemporal and inferonasal sectors, compared with PACG eyes, despite similar RNFL thicknesses in these sectors. These findings suggest that ocular perfusion change patterns differ between the two glaucoma subtypes.

The rates of RNFL thinning were detectable in the superotemporal, inferotemporal, and superonasal sectors of NTG eyes. Focal RNFL thinning in the superotemporal and inferotemporal sectors corresponds to the initial stages of optic nerve

damage in glaucomatous eyes. NTG eyes exhibited substantial VD loss over time in each sector and global region; such loss was more uniform than the observed RNFL thinning. These findings support the hypothesis that glaucomatous RNFL damage is a secondary consequence of insufficient ocular blood supply in NTG. Notably, our results may have been influenced by age-related changes. Based on the relatively short follow-up period, we believe that the rate of change is primarily disease related. Nonetheless, further longitudinal assessment is needed to clarify age-related changes in the VD and RNFL of healthy individuals.

Conclusion

This study provided evidence on the roles of retinal vascular changes in the pathogenesis of different glaucoma subtypes. Further studies are warranted to explore novel interventions based on vascular protection mechanisms.

Funding

This study was supported by the Health and Medical Research Fund, Health Bureau, Hong Kong SAR Government (#05162836). The full report is available from the Health and Medical Research Fund website (<https://rfs2.healthbureau.gov.hk>).

Disclosure

The results of this research have been previously published in:

1. Lin TPH, Hui HYH, Ling A, et al. Risk of normal tension glaucoma progression from automated baseline retinal-vessel caliber analysis: a prospective cohort study. *Am J Ophthalmol* 2023;247:111-20.
2. Wang YM, Shen R, Lin TPH, et al. Optical coherence tomography angiography metrics predict normal tension glaucoma progression. *Acta Ophthalmol* 2022;100:e1455-e1462.
3. Shen R, Wang YM, Cheung CY, et al. Relationship between macular intercapillary area measured by optical coherence tomography angiography and central visual field sensitivity in normal tension glaucoma. *Br J Ophthalmol* 2023;107:816-22.
4. Shen R, Wang YM, Cheung CY, Chan PP, Tham CC. Comparison of optical coherence tomography angiography metrics in primary angle-closure glaucoma and normal-tension glaucoma. *Sci Rep* 2021;11:23136.

References

1. Tham YC, Li X, Wong TY, Quigley HA, Aung T, Cheng

- CY. Global prevalence of glaucoma and projections of glaucoma burden through 2040: a systematic review and meta-analysis. *Ophthalmology* 2014;121:2081-90.
2. Leske MC, Wu SY, Hennis A, Honkanen R, Nemesure B; BESS Study Group. Risk factors for incident open-angle glaucoma: the Barbados Eye Studies. *Ophthalmology* 2008;115:85-93.
 3. Armaly MF, Krueger DE, Maunder L, et al. Biostatistical analysis of the collaborative glaucoma study. I. Summary report of the risk factors for glaucomatous visual-field defects. *Arch Ophthalmol* 1980;98:2163-71.
 4. Wu R, Cheung CY, Saw SM, Mitchell P, Aung T, Wong TY. Retinal vascular geometry and glaucoma: the Singapore Malay Eye Study. *Ophthalmology* 2013;120:77-83.
 5. Flammer J, Orgul S, Costa VP, et al. The impact of ocular blood flow in glaucoma. *Prog Retin Eye Res* 2002;21:359-93.